ELSEVIER

Journal of Alloys and Compounds 426 (2006) 286–289

Journal of ALLOYS AND COMPOUNDS

www.elsevier.com/locate/jallcom

# Synthesis and characteristics of $SnO_2$ needle-shaped nanostructures

Hyoun Woo Kim *, Seung Hyun Shim

*School of Materials Science and Engineering, Inha University, Incheon 402-751, Republic of Korea*

Received 8 November 2005; accepted 10 January 2006
Available online 29 March 2006

**Abstract**

We have demonstrated the synthesis of needle-shaped tin oxide ($SnO_2$) nanostructures by thermal evaporation of Sn powders. We have characterized the products with scanning electron microscopy, X-ray powder diffraction, transmission electron microscopy, and photoluminescence spectroscopy. The one-dimensional nanostructures, which gradually becomes thinner to form a sharp tip, appeared to be single crystals and had preferred [1 1 0] growth directions. Photoluminescence spectrum showed the visible light emission.


*PACS:* 81.07.-b

*Keywords:* $SnO_2$; Nanoneedles; Thermal evaporation



## 1. Introduction

Tin oxide ($SnO_2$), an important and inexpensive semiconductor with a wide band gap ($E_g = 3.62$ eV, at room temperature), is well known for its potential applications in gas sensors [1], transparent conducting electrodes [2], flat display devices [3], and solar cells [4]. While semiconductor crystals can be obtained in the nanometer length scale in various geometries [5,6], the one-dimensional (1D) variants warrant special attention because the anisotropy in quantum confinement potentials can be used to produce unusual optical, magnetic, and electronic properties [7,8]. Accordingly, various structural and morphological forms of 1D $SnO_2$ materials have been fabricated over the past several years, including nanowires [9–11], nanoribbons or nanobelts [12–17], nanorods [18–20], and nanotubes [21].

One of the most interesting and urgent challenges is the fabrication of 1D material with a novel morphology. Preparation of the nanoneedle is important not only for scientific interests but also for future industrial applications. For example, it has been observed that that the needle-like nanostructures with sharp tips significantly improve the field emission qualities [22,23]. However, to the best of our knowledge, no reports about the needle-shaped nanostruture of $SnO_2$ have been found. In the present work, we report on the synthesis of $SnO_2$ needle-shaped nanostructures by a simple evaporation route, their structural characterization, and also their photoluminescence (PL) spectrum.

## 2. Experimental

An alumina boat with the Sn powders (purity: 99.9%) was placed into a quartz tube in a furnace. We used thermally grown $SiO_2$ on Si(0 0 1) as a starting material onto which a layer of iridium (Ir) (about 150 nm) was deposited. On top of the boat, a piece of the substrate was placed with the Ir-coated side downwards. The powder-to-substrate distance was approximately 10 mm. During the experiment, a constant pressure with an air flow was maintained at 150 mTorr. The temperature of the furnace was increased to 900 °C from room temperature and kept at 900 °C for 2 h. After evaporation, the substrate was cooled down and then removed from the furnace for structural characterization. A white layer was found on the surface of the substrate.

The morphologies and crystal structure of the products were characterized using grazing angle X-ray diffraction (XRD: Cu $K\alpha_1$ radiation) (Philips X'pert MRD) with an incidence angle of 0.5° and scanning electron microscopy (SEM, Hitachi S-4200). Further structural analysis of individual nanostructure was performed using transmission electron microscopy (TEM, Philips CM-200). The PL measurement was performed at room temperature using a He–Cd laser (Kimon, 1K, Japan) line of 325 nm as the excitation source.

## 3. Results and discussion

Fig. 1a shows the plan-view SEM image, indicating that the 1D nanostructures are the dominant morphology in the top part of the product, although some irregularly shaped clusters are also

* Corresponding author. Tel.: +82 32 860 7544; fax: +82 32 862 5546.
*E-mail address:* hwkim@inha.ac.kr (H.W. Kim).

0925-8388/$ – see front matter © 2006 Elsevier B.V. All rights reserved.
doi:10.1016/j.jallcom.2006.01.093

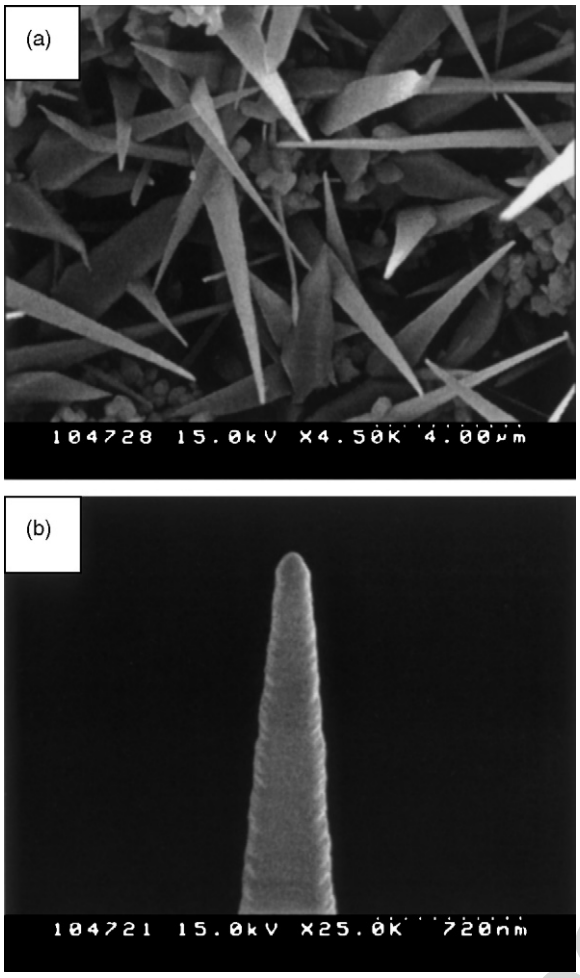


Fig. 1. (a) Top-view and (b) high magnification SEM images of the products.

found. Statistical observation of many SEM images indicates that the synthesized 1D nanostructures appear needle-shaped with the circular or rectangular cross-section and have sharp tips about 20–40 nm in width or diameter. Fig. 1b gives a high magnification SEM image, revealing that the diameter of the nanostructure decreases with increasing the length of the nanostructure from the bottom to the top, with no particle on the tip. The 1D nanostructure has an almost straight-line morphology.

The XRD pattern shown in Fig. 2 reveals the overall crystal structure of the products. The Miller indices are indicated on each diffraction peak. The diffraction peaks of the (1 1 0), (1 0 1), (2 0 0), (2 1 1), (2 2 0), (3 1 0), (1 1 2), (3 0 1) and (3 2 1) planes can be readily indexed to the tetragonal rutile structure of $SnO_2$ with lattice constants of $a = 4.7382$ Å and $c = 3.1871$ Å (JCPDS File No. 41-1445). No obvious reflection peaks from the impurities, such as unreacted Sn or other tin oxides, were detected, indicating the high purity of the products. In the XRD measurements, the angle of the incident beam to the substrate surface was approximately 0.5°, and the detector was rotated to scan the samples. Therefore, we surmise that the peaks are mainly from the products.

TEM is employed to further analyze the morphology of individual nanoneedles. Fig. 3a is a low magnification TEM image

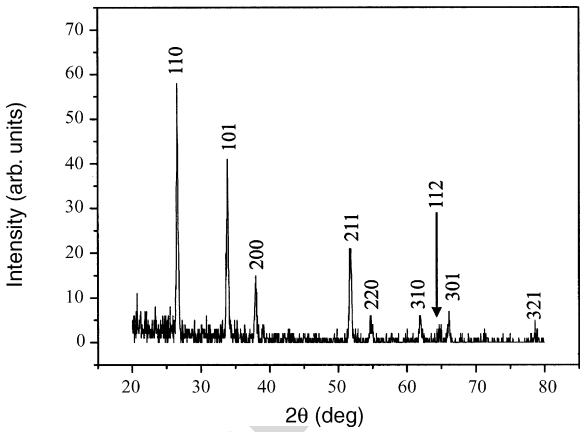


Fig. 2. XRD pattern recorded from the products.

of a single nanostructure, with its width gradually decreasing from bottom to the tip. The upper right inset in Fig. 3a shows an associated selected area electron diffraction (SAED) pattern from the single nanostructure with a [0 0 1] zone axis, which indicates that the as-prepared $SnO_2$ nanoneedles are single crystalline. Fig. 3b gives an enlarged TEM image showing an end portion of the nanostructure in Fig. 3a, which has an approximately 30 nm-wide tip with no spherical droplet or nanoparticle attached. Fig. 3c exhibits the high resolution TEM (HRTEM) image of the nanostructure shown in Fig. 3a. Lattice fringes are clearly visible from the HRTEM image, revealing its single crystalline nature. The lattice fringe distance is 0.33 nm, which is in coincidence with the (1 1 0) and (1 $\bar{1}$ 0) planes of the rutile $SnO_2$. It can be seen that the axis direction of the needle-shaped nanostructure is parallel to the [1 1 0] crystalline orientation of rutile $SnO_2$.

There are two well-accepted mechanisms for the growth of 1D nanostructures, the vapor–liquid–solid (VLS) and the vapor–solid (VS) mechanism. The VLS growth is a catalyst-assisted process, in which the metal catalyst particle acts as liquid-forming agent. In the present work, SEM and TEM images indicate that the nanoneedle tips are free of metal particles. Hence, VS mechanism may be more valid than the VLS one to demonstrate the growth of $SnO_2$ nanomaterials in the present synthesis route. While the temperature was elevated up to the reaction temperature, Sn source was continuously evaporated to form Sn vapor. A large amount of Sn vapor was transported to the substrate surface by the carrier gas, in which Sn atoms combined with O atoms. The oxygen in air is believed to provide the main source of oxygen for the growth of $SnO_2$ nanostructures.

Fig. 4a shows the side-view SEM image of the products. The needle-shaped 1D structures were grown on top of the cluster-like structures. Therefore, we deduce that the $SnO_2$ clusters were formed at an early stage of the synthesis process. When the synthesis was carried out under the same conditions at a lower substrate temperature in our previous experiments, the as-synthesized product showed a cluster-like morphology without any 1D structure (Fig. 4b) and thus it is possible that the cluster-like structures in this study (Fig. 4a) were formed while elevating the temperature during the heating process. Subsequently, the anisotropic growth behavior, producing $SnO_2$ nanostructures of

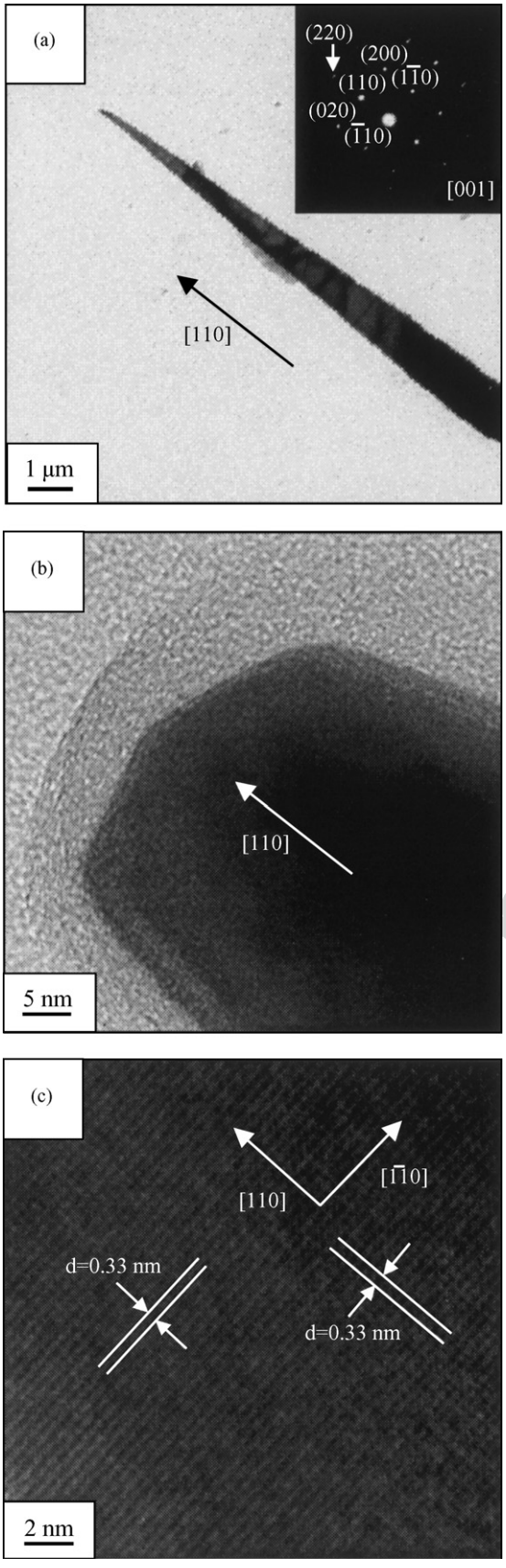


Fig. 3. (a) Low magnification TEM image of a needle-shaped nanostructure (inset: corresponding SAED pattern). (b) Enlarged TEM image representing the tip part of the nanostructure. (c) HRTEM image.

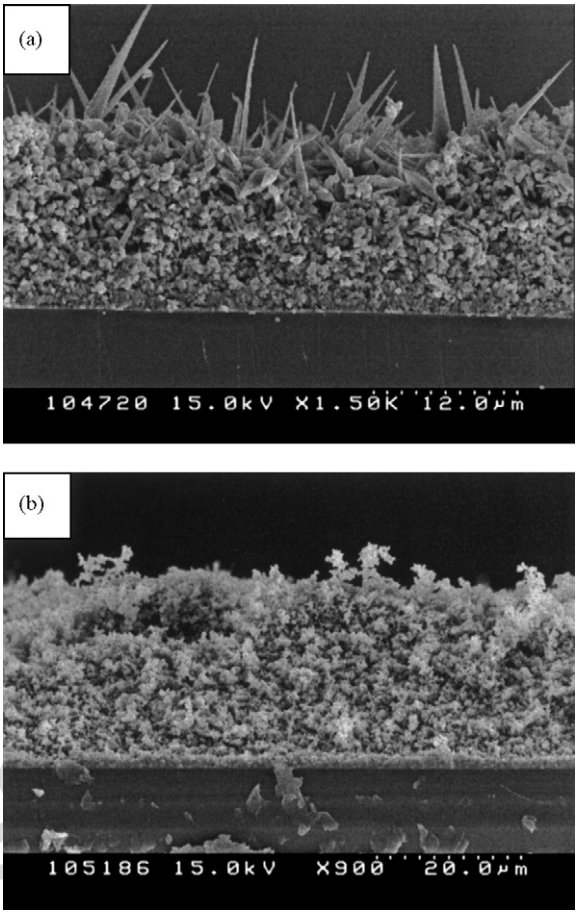


Fig. 4. Side-view SEM images of the products at a substrate temperature of (a) 900 and (b) 850 °C.

a high aspect ratio, may be enhanced at higher substrate temperature (900 °C), possibly due to the faster diffusion of Sn and O species. Considering the fact that the 1D structures in the present study grow via a VS process, we assume that the gradually diminishing Sn vapor supply could account for the eventual needle shape of the nanostructure. The reduction of Sn vapor supply may result from the exhaustion or surface oxidation of

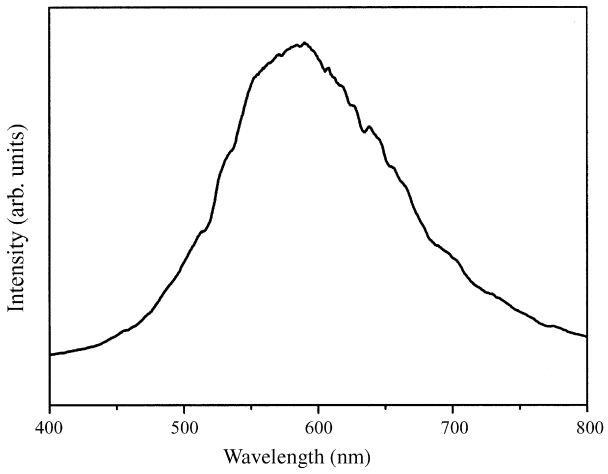


Fig. 5. Room temperature PL spectrum of the products with an excitation wavelength at 325 nm.

Sn powders. Similarly, several researchers attributed the formation of ZnO needle-like nanostructures to the reduction of Zn vapor source [24,25].

Fig. 5 shows a room temperature PL spectrum of the as-prepared products. There is an apparent broad emission PL band, with the dominant emission peak located at a wavelength of around 590 nm, corresponding to the energy of about 2.1 eV. A similar emission has been reported in the case of $SnO_2$ nanoribbons synthesized by laser ablation [26] and $SnO_2$ nanorods synthesized by solution phase growth [27]. The visible light emission is known to be related to crystal defects or defect levels within the band gap of $SnO_2$, associated with O vacancies or Sn interstitials that have formed during growth [26–28].

## 4. Conclusions

In summary, by a thermal evaporation method of heating Sn powders in air flow, we have fabricated a new form of needle-shaped $SnO_2$ nanostructures. We have characterized the samples by means of XRD, SEM, TEM, and PL spectroscopy. The $SnO_2$ nanoneedles with the rutile structure are single crystalline and have preferred [1 1 0] growth direction along the major axis. The room temperature PL spectrum under excitation at 325 nm shows a broad band with a prominent emission peak around 590 nm.

## Acknowledgement

This work was supported by Korea Research Foundation Grant (KRF-2004-003-D00141).

## References

[1] E.R. Leite, I.T. Weber, E. Longo, J.A. Varela, Adv. Mater. 12 (2000) 966.
[2] Y.S. He, J.C. Campbell, R.C. Murphy, M.F. Arendt, J.S. Swinnea, J. Mater. Res. 8 (1993) 3131.
[3] S.J. Laverty, P.D. Maguire, J. Vac. Sci. Technol. B 19 (2001) 1.
[4] S. Ferrere, A. Zaban, B.A. Gregg, J. Phys. Chem. B 101 (1997) 4490.
[5] A.P. Alivisatos, Science 271 (1996) 933.
[6] G. Markovich, C.P. Collier, S.E. Henrichs, F. Remacle, R.D. Levine, J.R. Heath, Acc. Chem. Res. 32 (1999) 415.
[7] J. Hu, T.W. Odom, C.M. Lieber, Acc. Chem. Res. 32 (1999) 435.
[8] Y. Cui, C.M. Lieber, Science 291 (2001) 851.
[9] M. Zheng, G. Li, X. Zhang, S. Huang, Y. Lei, L. Zhang, Chem. Mater. 13 (2001) 3859.
[10] A. Kolmakov, Y. Zhang, G. Cheng, M. Moskovits, Adv. Mater. 15 (2003) 997.
[11] J.K. Jian, X.L. Chen, T. Xu, Y.P. Xu, L. Dai, M. He, Appl. Phys. A 75 (2002) 695.
[12] Z.R. Dai, Z.W. Pan, Z.L. Wang, Solid State Commun. 118 (2001) 351.
[13] Z.L. Wang, Z.W. Pan, Adv. Mater. 14 (2002) 1029.
[14] J.Q. Hu, X.L. Ma, N.G. Shang, Z.Y. Xie, N.B. Wong, C.S. Lee, S.T. Lee, J. Phys. Chem. B 106 (2002) 3823.
[15] X.S. Peng, L.D. Zhang, G.W. Meng, Y.T. Tian, Y. Lin, B.Y. Geng, S.H. Sun, J. Appl. Phys. 93 (2003) 1760.
[16] X.L. Ma, Y. Li, Y.L. Zhu, Chem. Phys. Lett. 376 (2003) 794.
[17] S.H. Sun, G.W. Meng, Y.W. Wang, T. Gao, M.G. Zhang, Y.T. Tian, X.S. Peng, L.D. Zhang, Appl. Phys. A 76 (2003) 287.
[18] Y. Liu, C. Zheng, W. Wang, C. Yin, G. Wang, Adv. Mater. 13 (2001) 1883.
[19] C. Xu, G. Xu, Y. Liu, X. Zhao, G. Wang, Scripta Mater. 46 (2002) 789.
[20] D.-F. Zhang, L.-D. Sun, J.-L. Yin, C.-H. Yan, Adv. Mater. 15 (2003) 1022.
[21] Z.R. Dai, J.L. Gole, J.D. Stout, Z.L. Wang, J. Phys. Chem. B 106 (2002) 1274.
[22] Y.B. Li, Y. Bando, D. Golberg, Appl. Phys. Lett. 84 (2004) 3603.
[23] Y.W. Zhu, H.Z. Zhang, X.C. Sun, S.Q. Feng, J. Xu, Q. Zhao, B. Xiang, R.M. Wang, D.P. Yu, Appl. Phys. Lett. 83 (2003) 144.
[24] H.J. Fan, R. Scholz, A. Dadgar, A. Krost, M. Zacharias, Appl. Phys. A 80 (2005) 457.
[25] Y.-K. Tseng, C.-J. Huang, H.-M. Cheng, I.-N. Lin, K.-S. Liu, I.-C. Chen, Adv. Fund. Mater. 13 (2003) 811.
[26] J. Hu, Y. Bando, Q. Liu, D. Golberg, Adv. Funct. Mater. 13 (2003) 493.
[27] B. Cheng, J.M. Russell, W. Shi, L. Zhang, E.T. Samulski, J. Am. Chem. Soc. 126 (2004) 5972.
[28] S.-S. Chang, D.K. Park, Mater. Sci. Eng. B 95 (2002) 55.